

Hot electron plasmon-protected solar cell

J. Kong, A. H. Rose, C. Yang, X. Wu, J. M. Merlo, M. J. Burns, M. J. Naughton, and K. Kempa*

Department of Physics, Boston College, Chestnut Hill, Massachusetts 02467, USA

*kempa@bc.edu

Abstract: A solar cell based on a hot electron plasmon protection effect is proposed and made plausible by simulations, non-local modeling of the response, and quantum mechanical calculations. In this cell, a thin-film, plasmonic metamaterial structure acts as both an efficient photon absorber in the visible frequency range and a plasmonic resonator in the IR range, the latter of which absorbs and protects against phonon emission the free energy of the hot electrons in an adjacent semiconductor junction. We show that in this structure, electron–plasmon scattering is much more efficient than electron–phonon scattering in cooling-off hot electrons, and the plasmon-stored energy is recoverable as an additional cell voltage. The proposed structure could become a prototype of a new generation of high efficiency solar cells.

© 2015 Optical Society of America

OCIS codes: (240.6680) Surface plasmons; (350.6050) Solar energy; (250.5403) Plasmonics; (350.4238) Nanophotonics and photonic crystals; (160.4236) Nanomaterials; (310.6628) Subwavelength structures, nanostructures.

References and links

1. J. B. Gunn, “Microwave oscillations of current in III–V semiconductors,” *Solid State Commun.* **1**(4), 88–91 (1963).
2. R. T. Ross and A. J. Nozik, “Efficiency of hot-carrier solar energy converters,” *J. Appl. Phys.* **53**(5), 3813–3818 (1982).
3. H. Kroemer, “Theory of the Gunn effect,” *Proc. IEEE* **52**(12), 1736 (1964).
4. D. Frohman-Bentchkowsky, “Memory behavior in a floating-gate avalanche-injection MOS (FAMOS) structure,” *Appl. Phys. Lett.* **18**(8), 332–334 (1971).
5. M. Heiblum, M. I. Nathan, D. C. Thomas, and C. M. Knoedler, “Direct observation of ballistic transport in GaAs,” *Phys. Rev. Lett.* **55**(20), 2200–2203 (1985).
6. C. Rauch, G. Strasser, K. Unterrainer, W. Boxleitner, K. Kempa, and E. Gornik, “Ballistic electron transport in vertical biased superlattices,” *Physica E* **2**(1–4), 282–286 (1998).
7. A. Othonos, “Probing ultrafast carrier and phonon dynamics in semiconductors,” *J. Appl. Phys.* **83**(4), 1789–1830 (1998).
8. J. R. Goldman and J. A. Prybyla, “Ultrafast dynamics of laser-excited electron distributions in silicon,” *Phys. Rev. Lett.* **72**(9), 1364–1367 (1994).
9. S. M. Sze, *High-Speed Semiconductor Devices* (Wiley, 1990).
10. K. M. Kramer and W. N. G. Hitchon, *Semiconductor Devices: A Simulation Approach* (Prentice Hall, 1997).
11. J. A. Kash and J. C. Tsang, “Watching chips work: Picosecond hot electron light emission from integrated circuits,” *J. Cryst. Growth* **210**(1–3), 318–322 (2000).
12. W. Shockley and H. J. Queisser, “Detailed balance limit of efficiency of *p-n* junction solar cells,” *J. Appl. Phys.* **32**(3), 510–519 (1961).
13. M. A. Green, *Third Generation Photovoltaics: Advanced Solar Energy Conversion* (Springer, 2006).
14. K. Kempa, “Plasmonic protection of the hot-electron energy,” *Phys. Status Solidi RRL* **7**(7), 465–468 (2013); (erratum) *ibid* **7**(12), 1112 (2013).
15. P. C. Cheng, “The contrast formation in optical microscopy,” in J. B. Pawley (ed.) *Handbook of Biological Confocal Microscopy*, 3rd edn. (Springer, 2006), pp. 162–206.
16. C. Clavero, “Plasmon-induced hot-electron generation at nanoparticle/metaloxide interfaces for photovoltaic and photocatalytic devices,” *Nat. Photonics* **8**(2), 95–103 (2014).
17. H. Chalabi and M. L. Brongersma, “Plasmonics: harvest season for hot electrons,” *Nat. Nanotechnol.* **8**(4), 229–230 (2013).
18. M. L. Brongersma, N. J. Halas, and P. Nordlander, “Plasmon-induced hot carrier science and technology,” *Nat. Nanotechnol.* **10**(1), 25–34 (2015).

19. D. J. Farrell, H. Sodabanlu, Y. Wang, M. Sugiyama, and Y. Okada, "Can a hot-carrier solar cell also be an efficient up-converter?" *IEEE J. Photovoltaics* **5**(2), 571–576 (2015).
20. G. L. Liu, Y. T. Long, Y. Choi, T. Kang, and L. P. Lee, "Quantized plasmon quenching dips nanospectroscopy via plasmon resonance energy transfer," *Nat. Methods* **4**(12), 1015–1017 (2007).
21. G. D. Mahan, *Many-Particle Physics* (Plenum, 1981).
22. J. J. Quinn and R. A. Ferrell, "Electron self-energy approach to correlation in a degenerate electron gas," *Phys. Rev.* **112**(3), 812–827 (1958).
23. R. D. Mattuck, *A Guide to Feynman Diagrams in the Many-Body Problem* (McGraw-Hill, 1976).
24. O. D. Restrepo, K. Varga, and S. T. Pantelides, "First-principles calculations of electron mobilities in silicon: Phonon and Coulomb scattering," *Appl. Phys. Lett.* **94**(21), 212103 (2009).
25. D. Rideau, W. Zhang, Y. M. Niquet, C. Delerue, C. Tavernier, and H. Jaouen, "Electron-phonon scattering in Si and Ge: From bulk to nanodevices," *2011 International Conference on Simulation of Semiconductor Processes and Devices (SISPAD) Conference Publication* (2011) pp. 47–50.
26. Y. Wang, T. Sun, T. Paudel, Y. Zhang, Z. Ren, and K. Kempa, "Metamaterial-plasmonic absorber structure for high efficiency amorphous silicon solar cells," *Nano Lett.* **12**(1), 440–445 (2012).
27. F. Ye, M. J. Burns, and M. J. Naughton, "Embedded metal nanopatterns as a general scheme for enhanced broadband light absorption," *Phys. Status Solidi A* **212**(3), 561–565 (2015).
28. F. Ye, M. J. Burns, and M. J. Naughton, "Embedded metal nanopatterns for near-field scattering-enhanced optical absorption," *Phys. Status Solidi A* **209**, 1829–1834 (2012).
29. A. Taflove, *Computational Electrodynamics: The Finite-Difference Time-Domain Method* (Artech House, 1995) Norwood, MA.
30. X. Wang and K. Kempa, "Negative refraction and subwavelength lensing in a polaritonic crystal," *Phys. Rev. B* **71**(23), 233101 (2005).
31. www.cst.com.
32. A. F. Oskooi, D. Roundy, M. Ibanescu, P. Bermel, J. D. Joannopoulos, and S. G. Johnson, "MEEP: A flexible free-software package for electromagnetic simulations by the FDTD method," *Comput. Phys. Commun.* **181**(3), 687–702 (2010).
33. M. Scharte, R. Porath, T. Ohms, M. Aeschlimann, J. R. Krenn, H. Ditlbacher, F. R. Aussenegg, and A. Liebsch, "Do Mie plasmons have a longer lifetime on resonance than off resonance?" *Appl. Phys. B* **73**(4), 305–310 (2001).
34. O. S. Heavens, *Optical Properties of Thin Solid Films* (Dover, 1965).
35. P. J. Feibelman, "Microscopic calculation of electromagnetic fields in refraction at a jellium-vacuum interface," *Phys. Rev. B* **12**(4), 1319–1336 (1975).
36. P. J. Feibelman, "Surface electromagnetic fields," *Prog. Surf. Sci.* **12**(4), 287–407 (1982).
37. A. Liebsch, "Dynamical screening at simple-metal surfaces," *Phys. Rev. B Condens. Matter* **36**(14), 7378–7388 (1987).
38. K. Kempa, A. Liebsch, and W. L. Schaich, "Comparison of calculations of dynamical screening at jellium surfaces," *Phys. Rev. B Condens. Matter* **38**(17), 12645–12648 (1988).
39. A. Liebsch, "Surface-plasmon dispersion and size dependence of Mie resonance: Silver versus simple metals," *Phys. Rev. B Condens. Matter* **48**(15), 11317–11328 (1993).
40. P. B. Johnson and R. W. Christy, "Optical constants of the noble metals," *Phys. Rev. B* **6**(12), 4370–4379 (1972).
41. M. W. Knight, H. Sobhani, P. Nordlander, and N. J. Halas, "Photodetection with active optical antennas," *Science* **332**(6030), 702–704 (2011).
42. K. Kempa, M. J. Naughton, Z. Ren, A. Herczynski, T. Kirkpatrick, J. Rybczynski, and Y. Gao, "Hot electron effect in nanoscopically thin photovoltaic junctions," *Appl. Phys. Lett.* **95**(23), 233121 (2009).
43. F. Wang and N. A. Melosh, "Plasmonic energy collection through hot carrier extraction," *Nano Lett.* **11**(12), 5426–5430 (2011).
44. F. Wang and N. A. Melosh, "Power-independent wavelength determination by hot carrier collection in metal-insulator-metal devices," *Nat. Commun.* **4**, 1711 (2013).

1. Introduction

Charge carriers in semiconductors having excess energy (*i.e.* above the conduction band minimum for electrons and below the valence band maximum for holes) are referred to as "hot". For example, electrons photoexcited from a valence band deep into a conduction band are considered hot electrons. Effects of hot electrons have been studied and utilized for more than half a century in a variety of electronic devices, from Gunn diodes to integrated circuits [1–11]. In conventional solar cells, hot electrons rapidly and irreversibly lose their excess energy (defined as the difference between the energies of their occupied states and that of the bottom of the conduction band, with a similar relationship for holes and the valence band) to phonons (heat) [2], which leads to the Shockley-Queisser limit for single junction cell efficiency [12]. The amount of the energy lost to heat in a conventional cell often exceeds that harvested in the form of electricity. For example, commercially available, high efficiency

crystalline silicon solar cells convert 20-25% of absorbed sunlight into electricity, but more than 30% into heat via hot electrons. Many concepts have been proposed to harvest or convert this hot electron energy into usable form, but none have been experimentally verified or demonstrated to date [13].

Recently, a scheme was proposed to reduce the number of irreversibly dissipative electron-phonon scattering events in a solar cell, by providing an energy-dissipation channel into plasmons in an adjacent or embedded plasmonic structure [14]. In this scheme, the hot electron free energy remains reversibly “protected” in a collective electronic degree of freedom. This hot electron plasmon protection (HELPP) mechanism, which relies on electron-plasmon scattering occurring on a time scale sufficiently smaller than phonon emission by either plasmons or hot electrons, was theoretically supported by a simple model calculation [14]. The effect is somewhat similar to the Förster resonance energy transfer (FRET) known in molecular physics, describing non-radiative (dipole-dipole) energy transfer between an excited electronic state of a donor molecule and single electron excitation of a nearby acceptor molecule [15]. It is distinct from schemes in which subgap photons are absorbed by a plasmonic metal followed by energy transfer to a semiconductor [16–18], as well as from up-conversion mechanisms [19]. HELPP can also be viewed as an inverse of plasmon resonance energy transfer (PRET) [20], where localized plasmon oscillations in metallic nanoparticles non-radiatively excite electrons in adjacent (a few nanometers away) molecules.

Here, we confirm by detailed simulations that the HELPP mechanism can be achieved in an ultrathin metamaterial structure, which acts simultaneously as a plasmonic resonator in the infrared (IR) and a broad-band visible absorber. Electrically disconnecting the two could lead to a tandem hot electron photovoltaic device in which the absorber acts as a conventional solar cell, and the plasmonic resonator (which stores the hot electron energy) could be made a part of a Schottky cell, yielding an additional voltage originating from the hot electron energy.

2. Theoretical model

In general, the scattering rate of an electron excited in a semiconductor from a state E_k to states E_{k+q} , due to single particle and collective (plasmon) excitations (with wave vectors \mathbf{q}), is given by [21–23]

$$\gamma_k \approx -\frac{2}{\hbar} \int \frac{d\mathbf{q}}{(2\pi)^3} \left[n_B(E_k - E_{k+q}) - n_F(-E_{k+q} + \mu) \right] \text{Im} \left[V_{\text{eff}} \left[\mathbf{q}, (E_{k+q} - E_k) / \hbar \right] \right], \quad (1)$$

where n_B and n_F are the Bose-Einstein and Fermi-Dirac distribution functions, respectively, μ is the chemical potential, and $V_{\text{eff}}(\mathbf{q}, \omega)$ is the dressed combined interaction. This latter term can be written as a simple (but exact) sum of the Coulomb and phonon (Fröhlich) terms [23],

$$V_{\text{eff}}(\mathbf{q}, \omega) = \frac{V_q}{\varepsilon(\mathbf{q}, \omega)} + \frac{\Omega_q |\mathbf{g}_q / \varepsilon(\mathbf{q}, \omega)|^2}{\omega^2 - \Omega_q^2 / \varepsilon(\mathbf{q}, \omega) + i0^+}, \quad (2)$$

where $\varepsilon(\mathbf{q}, \omega)$ is the longitudinal dielectric function of the medium, \mathbf{g}_q is the matrix element, V_q is the bare Coulomb interaction, and Ω_q is the longitudinal phonon frequency (plasma frequency of the ionic “plasma”). Equation (2) is written in the random phase approximation for electrons (1st term), and the point-ion, long wavelength approximation for ions (2nd term). The simple, additive form of Eq. (2) allows one to write the total scattering rate as $\gamma_k = \gamma_{el-pl} + \gamma_{el-ph}$, where γ_{el-pl} is given by Eq. (1) with $V_{\text{eff}}(\mathbf{q}, \omega)$ given by only the first (Coulomb) term in Eq. (2), and γ_{el-ph} given by only the second (Fröhlich) term. Here, the subscripts *el*, *ph*, and *pl* refer to electron, phonon and plasmon, respectively. Since γ_{el-ph} for

systems of interest here has been studied in detail elsewhere [24,25], we focus on calculating only γ_{el-pl} .

Clearly, this calculation requires knowledge of the effective dielectric function of a given structure. In Ref [14], a simple model structure was considered in which a semiconductor film was assumed to be coupled so strongly to a metallic, plasmonic resonator that the system could be described as an “effective medium” with an effective relative dielectric function of the general form:

$$\varepsilon(\omega) = \varepsilon_b + \sum_{m=1}^M \frac{\omega_{pm}^2}{\omega_{rm}^2 - \omega(\omega + i\bar{\gamma}_{el-ph}) - \Sigma(q)}, \quad (3)$$

where it was assumed for simplicity that $M = 1$ (only one, dominant plasmon resonance), and the self-energy $\Sigma(q)$ and the electron-phonon scattering rate in the metal vanish ($\Sigma(q) = 0$ and $\bar{\gamma}_{el-ph} \rightarrow 0^+$). Here, each plasmon resonance, indexed by mode m , is characterized by a modal plasma frequency ω_{pm} and a localized plasmon modal resonance frequency ω_{rm} within the Drude-Lorentz model and ε_b is the core or bound electron dielectric constant. When Eq. (3) is inserted into Eqs. (1) and (2), calculations [14] showed that plasmon emission by a hot electron in a semiconductor could occur at the rate of $\gamma_{el-pl} \approx 10^{14} \text{ s}^{-1}$, which is faster than the typical phonon emission rate in the semiconductor, $\gamma_{el-ph} \approx 10^{13} \text{ s}^{-1}$. In such a case, the hot electron “cools down” to the bottom of the conduction band by emitting plasmons in the collector/plasmon resonator, rather than by emitting phonons in the semiconductor medium. However, this is a necessary but not sufficient condition for the HELPP effect to occur. In addition, one must arrange for the plasmons in the metal to decay into phonons sufficiently slowly. This indeed is expected to be the case, since typical plasmon-phonon scattering rates in metals are $\gamma_{pl-ph} \approx \bar{\gamma}_{el-ph} \approx 10^{13} \text{ s}^{-1}$.

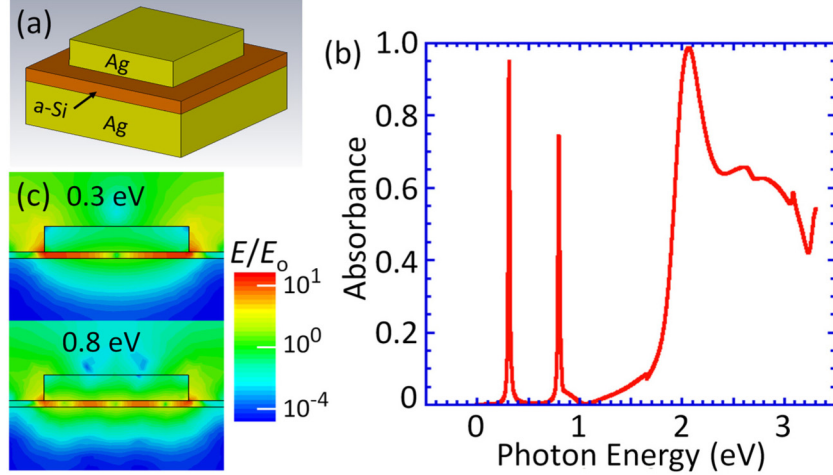


Fig. 1. (a) Schematic of a unit cell ($300 \text{ nm} \times 300 \text{ nm}$) of a square array of plasmonic resonators in a HELPP solar cell structure. The thickness of each layer is: macroscopically-thick Ag bottom electrode, 10 nm $a\text{-Si}$ absorber, and 40 nm Ag top plasmonic resonator ($200 \text{ nm} \times 200 \text{ nm}$). (b) Simulated absorbance spectrum of the structure, showing two plasmon resonances in the infrared. For the purposes of this paper, this scale for the resonance peaks near 0.3 and 0.8 eV refers to energies above (below) a semiconductor absorber’s conduction (valence) band edge. (c) Electric field distribution (scaled to the incident field magnitude) in a cross-section of the unit cell (through the unit center, parallel to the unit side), at the

frequencies of the main plasmon resonance peaks at 0.3 and 0.8 eV. Field enhancements up to $E/E_0 \sim 30$ (i.e. intensity gain $\sim 30^2 \sim 1,000$) are realized within the photovoltaic absorber.

It is clear that HELPP depends on strong interactions between the semiconductor, where the electron transitions occur, and the plasmonic resonator. This depends on, among other things, their relative proximity. PRET studies [20] have shown that one needs distances of the order of 10 nm to achieve strong coupling. Therefore, the semiconductor film, e.g. the active region of a solar cell, must be very thin, on a similar 10 nm scale. Solar cells of such thickness are indeed feasible; highly-efficient light trapping in active media of the order of 10 nm thickness has been demonstrated with plasmonic metamaterial schemes [26–28]. Here, we propose a solar cell based on such a scheme, modified to assure also a contribution from HELPP.

3. Simulation and calculation of scattering rates

We consider first a version of the solar cell which enables highly efficient light absorption and HELPP action, but not yet having optimized electronic recovery of the hot electron energy. A schematic of this basic HELPP structure is shown in Fig. 1(a), which is a unit cell of a periodic square array with lattice constant 300 nm. It consists of a metallic (Ag) back electrode, an active semiconductor layer (ultrathin *a*-Si *p-i-n* junction) of total thickness 10 nm, and a top, square metallic (Ag) plasmonic resonator with thickness 40 nm and side width 200 nm. The absorption spectrum of this structure, calculated by using the FDTD method [29–32] and intrinsic *a*-Si as the absorber, is shown in Fig. 1(b). It has a broad band in the visible frequency range that assures high photon absorption. This is the signature of the structure’s metamaterial action, similar to that reported in Refs [26–28]. The spectrum has also two sharp absorbance peaks in the infrared, near 0.3 eV and 0.8 eV; these are the plasmon resonances that enable the HELPP effect. The corresponding electric field distribution, calculated at the frequencies of those main plasmonic peaks, is shown in Fig. 1(c). Strong concentration of the field (intensity enhancement over incident value $(E/E_0)^2 \sim 30^2 \sim 10^3$) within the semiconductor film is clearly visible. These plasmon resonances are designed to be excited by hot electrons, and the excitation rate can be calculated from Eq. (1). However, photons from the IR tail of the solar spectrum could also directly excite these resonances, further improving the efficiency of a tandem configuration discussed below. We have also simulated the effect of positioning a point dipole directly in the absorber layer, and found that, as expected, this also excites the plasmon resonances in the IR, with comparable efficiency.

To calculate the various scattering rates in this structure, we need to obtain its aforementioned effective dielectric function. To achieve this, we first model the system as a three-layer problem: a semi-infinite Ag substrate, an effective coating of total thickness d , and vacuum. Such a model has been shown [33] to be a good approximation for the optical response of thin discontinuous films, provided that the effective dielectric function of the film is extended into the nonlocal domain, as discussed and applied below. The effective coating, which consists of the absorber and Ag nanostructures of Fig. 1(a), is described in the IR via a single effective dielectric function $\varepsilon(\omega)$ of the form of Eq. (3) with two Lorentzian terms ($M = 2$), associated with the two HELPP-enabling plasmon resonances of Fig. 1(b). The parameters of this Lorentzian expansion are chosen so that the reflectance R of the model three-layer system [34] closely fits that obtained from the simulation in Fig. 1(b),

$$R = |r|^2 = \left| \frac{(1 - \sqrt{\varepsilon}) - (1 + \sqrt{\varepsilon}) \exp(i4\pi nd / \lambda)}{(1 + \sqrt{\varepsilon}) + (1 - \sqrt{\varepsilon}) \exp(i4\pi nd / \lambda)} \right|^2. \quad (4)$$

Note that the simulated reflectance $R = 1 - A$ can be immediately obtained from the absorbance A in Fig. 1(b). The resulting fit is shown in Fig. 2(a) above, comparing well with calculations from the model.

Before using it to calculate the scattering rate, the local effective dielectric function $\varepsilon(\omega)$ obtained from the fit must be extended into the non-local domain, *i.e.* it must be made dependent on the wavevector q . This is because while the optical response is limited to only very small momenta, much less than the Fermi momentum ($q \ll k_F$), the plasmon scattering of hot electrons involves both small and large momentum transfers (q of order k_F). The most efficient way to accomplish this analytical extension is to use the D -function formalism of Feibelman [35, 36]. This combines the simplicity of the Fresnel analysis with a rigorous quantum mechanical treatment by introducing surface response functions $D(\omega)$, which have been systematically calculated for various metals [37, 38]. Liebsch [39] has shown that the self-energy in Eq. (3) can be expressed in terms of the Feibelman D as:

$$\Sigma(q) = |q|D(\omega)\omega_s^2 \approx |q|D(\omega_s)\omega_s^2, \quad (5)$$

$$\omega_s = \omega_p / \sqrt{1 + \text{Re}(\varepsilon_b)}, \quad (6)$$

where ω_s is the surface plasmon frequency, and Eq. (5) is inserted into Eq. (3) to yield the non-locally extended dielectric function, which subsequently is inserted into Eqs. (1) and (2) to yield γ_{el-pl} , shown in Fig. 2(b). Due to the simplicity of the Lorentzian formula, part of Eq. (1) can be done analytically. One result shown (in red, marked “min”) could be considered a worst-case scenario, using the largest possible value of the only adjustable parameter, $\varepsilon_b = 10$, which assumes that ε_b equals the maximum bulk value in silver [40]. We also show a more realistic scenario range (in blue, marked “max”) which uses a bulk vacuum-weighted background dielectric constant of $\varepsilon_b = 3$.

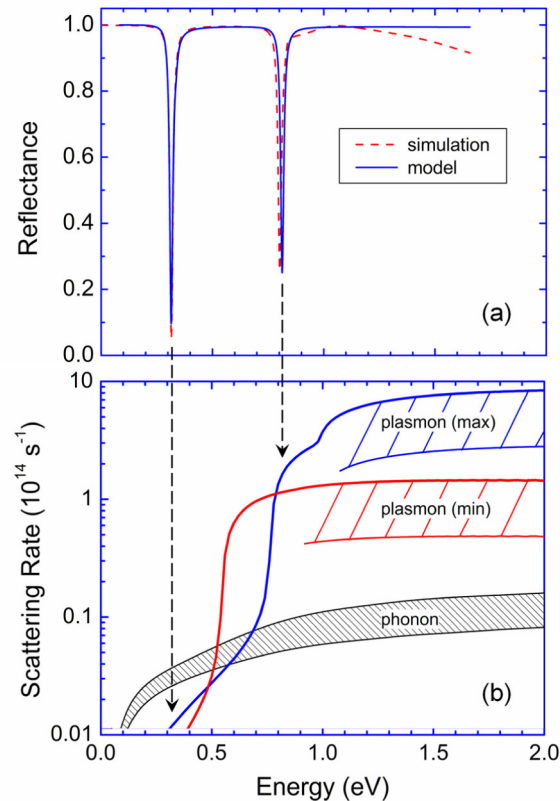


Fig. 2. (a) Reflectance of the structure shown in Fig. 1: simulations (dashed line) and model three-layer system calculations (solid line). (b) Calculated minimum (red) and maximum (blue)

ranges of scattering rates for hot electrons with plasmons (corresponding to the upper and lower limits, respectively, for the background permittivity), and the reported range of scattering rates [24,25] for hot electrons with phonons (black). Arrows indicate connections between plasmonic absorbance resonances and enhancements in hot electron-plasmon scattering.

Finally, these ranges can be compared to a range for the electron-phonon scattering rate, obtained from Refs [24,25]. Figure 2(b) demonstrates that in the typical range of hot electron energies (say, 0.7 – 2 eV, corresponding to the energy range of solar radiation minus a typical PV absorber band gap) one has at least $\gamma_{el-pl} / \gamma_{el-ph} > 1$ (though it could reach $\sim 10^2$, Fig. 2(b)), broadly confirming the earlier, simple model result. Throughout, we refer to the hot electron energy E_{hot} as that in excess of the conduction band minimum. The most important feature for the HELPP effect is the *hot-electron relaxation* (*i.e. complete cooling-off*) time, τ^c ; this is the time required to cool a hot electron from its initial, high photoexcited energy state down to the bottom of the conduction band. This time depends on the quantum energy exchanged at each scattering event. While the typical phonon energy is in the 50 meV range, the plasmon energy is a few hundred meV, and so about factor of ten larger. Therefore, it takes about 10 times fewer plasmon scattering events than phonon events to completely cool off a hot electron. Taking this effect into account, we estimate that for an average hot-electron energy of about 1 eV, which coincides with $\gamma_{el-pl} / \gamma_{el-ph} \gg 1$, the corresponding cooling time ratio is $\tau_{el-pl}^c / \tau_{el-ph}^c \ll 1$. Thus, *electron-plasmon scattering dominates carrier relaxation*.

4. Application to photovoltaics

With a PV junction representing the semiconductor film, the structure of Fig. 1(a), after coating with a transparent conductor, is a functioning solar cell, with the periodic, plasmonic structure also acting as one charge collector of the cell. The HELPP action will lead to an increased voltage of the cell relative to that without HELPP. To see this, consider a hot electron generated in the conduction band of the semiconductor, as in Fig. 3(a). In the absence of HELPP, this electron would first lose its entire free energy to phonon scattering on a femtosecond time scale, and then, as it drifts towards the collector, would continue to thermalize with the lattice, as well as with other electrons. With HELPP, the process is similar, except the initial “cooling” of the electron occurs via plasmon emission, with the plasmons resonating in the plasmonic collector, Fig. 3(b). Any electron arriving at the metallic plasmonic collector rejoins the free-energy stored initially in the form of a plasmon. These plasmons rapidly undergo Landau damping (LD), *i.e.*, they turn into single particle excitations (electron-hole pairs), such that the plasmon energy turns into the electron-hole pair energy, Fig. 3(b). This damping is rapid, comparable to that of plasmon-electron scattering [33, 41], such that the hot electron energy remains in the electronic degree of freedom, *i.e.* is protected from phonon emission. Initially photoexcited electrons arriving at the collector recombine with the hole of this electron-hole pair, Fig. 3(c), and an excited hot-electron in the collector is the final product of the process, Fig. 3(d). The end result is thus identical to that of *a hot-electron never losing its free energy on its way to the collector*.

HELPP, therefore, is a mechanism that effectively extends the lifetime (or the mean free path) of a hot electron. In recent work, it was demonstrated that in ultrathin *p-i-n a-Si* junctions, hot electrons contributed to small voltage increase to the overall open circuit voltage [42]. We anticipate a similar but significantly stronger effect to be observable in the proposed HELPP structure.

The efficiency of this effect can potentially be improved by modifying the structure so that the plasmonic resonators are electrically separated from the semiconductor. This can be achieved by placing a very thin dielectric spacer between the semiconductor and the array of metallic resonators (red layer in the schematic in Fig. 4). This should eliminate any deleterious, direct electron-electron scattering between the electrons in the semiconductor and the plasmonic reservoir, making the HELPP effect much stronger. The hot-electron energy

stored in the plasmonic reservoirs can potentially be detected via small radiation resulting from the plasmon resonators, or can be directly extracted from the generated LD electron-hole pairs. These can be spatially separated in a metal-insulator-metal (MIM) structure [43, 44], or at Schottky barriers formed at the interface of the plasmonic nanostructures and the semiconductor [41]. In either case, an electron of the LD electron-hole pair is excited above the asymmetric potential barrier, leaving behind a hole in the nanostructure, and producing a contact voltage due to separation of the carriers. As such, one could prepare a type of *tandem, high efficiency hot electron cell*, as depicted in Fig. 4. The first cell of this tandem is our basic HELPP cell shown in Fig. 1, but with an insulating spacer between the PV junction and the Ag plasmonic resonators (thick red layer), as well as ITO. This cell would produce the conventional photovoltage, as indicated in the band diagram in Fig. 5. The second cell consists of the plasmonic reservoir array coated with a thin semiconductor (e.g. *n*-type Si or *a*-Si) to form a Schottky barrier with the metal of the reservoir and ITO. This cell produces a voltage that is directly proportional to the hot electron energy. Connected in series, this tandem combination would lead to a hot electron solar cell with efficiency exceeding the Shockley-Queisser limit. Current matching can be achieved simply by controlling the surface area of each cell in the tandem.

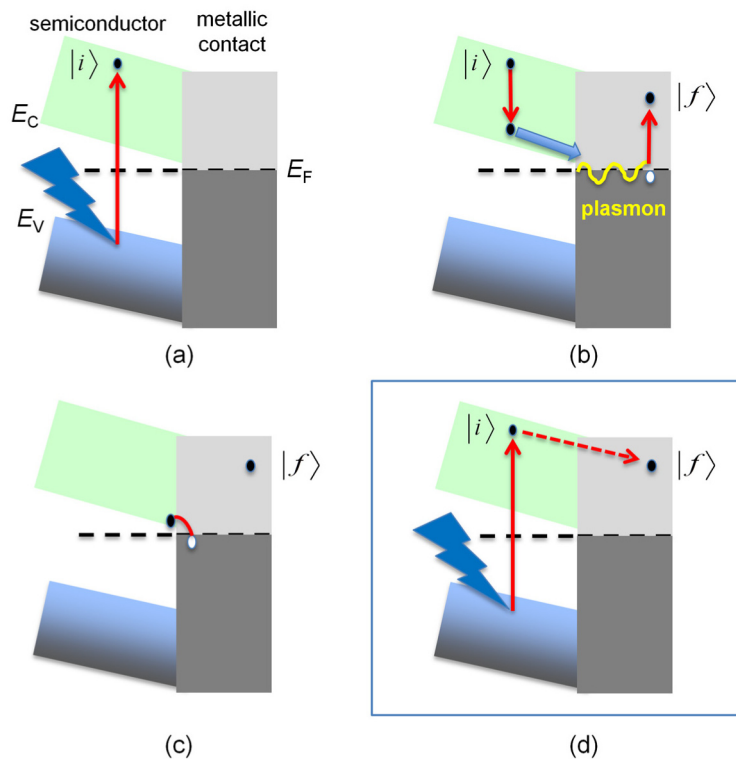


Fig. 3. Schematic of HELPP action. (a) A semiconductor absorbs a photon of energy greater than the band gap $E_C - E_V$, exciting an electron high into the conduction band. (b) Prior to losing the above-gap excess energy to phonons/heat, this hot electron resonantly exchanges that excess energy with a plasmon mode in a proximate plasmonic metamaterial structure having effective Fermi energy E_F . This plasmon Landau damps into an electron-hole pair in the metal (e.g. Ag). (c) The originally photoexcited electron recombines with the plasmon-excited hole at E_F , leaving behind a high energy electron to be harvested as current, and at higher voltage than that conventionally determined by the semiconductor band gap. These 3 steps can equivalently be described by the process in (d).

